

# Monitoring optical properties of apple tissue during cool storage

Laszlo Baranyai, Christian Regen, Manuela Zude

Leibniz-Institut für Agrartechnik Potsdam-Bornim e.V., Max-Eyth-Allee 100, 14469 Potsdam, Germany

Corresponding author: lbaranyai@atb-potsdam.de

**Abstract:** Apples (*Malus domestica*) of 'Elstar' and 'Pinova' of three different ripeness stages (unripe, ripe and overripe) were stored in separate chambers with 2°C and controlled atmosphere (2% CO<sub>2</sub>, 1.5% O<sub>2</sub>) between August 2008 and March 2009. During storage, 30 pieces of each cultivar were randomly selected for one measurement. Monochrome camera (JAI A50IR CCIR, JAI, Denmark) was used to capture images of 720x576 pixel size with 0.1694 mm/pixel resolution. The selected point on the apple surface was illuminated with circular laser beam of 7° incident angle and 785 nm wavelength (LPM785-45C, Newport Corp., USA). The vision system was controlled using LabView 8.6 PDS (National Instruments, USA) software extended with a dynamic library including image processing functions. The observed spatial distribution of intensity was used to estimate optical properties of fruit tissue. Backscattering profiles were computed based on radial averaging relative to the incident point. The logistic shape of the collected profiles was analyzed further to estimate optical properties such as absorption coefficient ( $\mu_a$ ), scattering ( $\mu_s$ ) and anisotropy factor ( $g$ ). The size of the total backscattering area was also taken into account to describe light penetration and distribution in apple tissue. The method appears reasonable for characterising changes in the optical properties of fruit in postharvest.

## 1 Introduction

Investigation of interactions between light and biological materials is of great interest since optical methods provide non-destructive way of quality assessment and monitoring. Mechanical injury of bruising was detected on apples with visible/NIR spectroscopy methods utilizing wavebands around 545 nm and 1200 nm (XING *et al.* 2006). Soluble solids content (SSC) and acidity of 'Fuji' apples were measured using FT-NIR spectrometry in the wavelength range of 812–2357 nm (LIU & YING 2005). Hyperspectral imaging system with artificial neural network was trained and applied successfully to detect chilling injury of Red Delicious apples based on five wavelengths (717, 751, 875, 960 and 980 nm) (ELMASRY *et al.* 2009). This neural network estimated fruit firmness with 9.4 N root mean square error (RMSE) and obtained 98.4% classification accuracy. Decline in firmness of 'Sansa' apple during storage on room temperature (19-23°C) was

monitored with ultrasonic device (KIM *et al.* 2009). QIN & LU (2008) applied hyperspectral technique to analyze how absorption ( $\mu_a$ ) and light scattering ( $\mu_s'$ ) are correlated with ripeness of fruits and vegetables. Product specific  $\mu_a$  and  $\mu_s'$  spectra were calculated in the wavelength range of 500–1000 nm using the Farrell model. Additionally, based on the obtained optical parameters, the light penetration depth was also estimated for numerous horticultural produces. The internal structures of tissues, such as fibres, were found to affect light distribution and result in distortion of the measured intensity in certain directions (SVIRIDOV *et al.* 2005). Laser beam emitting at 650 nm was used to detect structures in bone and skin according to the distortion in light diffusion (SVIRIDOV *et al.* 2005).

The objective of the presented work was to estimate optical properties of apple tissue during controlled atmosphere cool storage using laser induced backscattering imaging. The selected optical properties include anisotropy factor ( $g \in ]-1, 1[$ ), which describes the probability of scattering directions.

## 2 Materials and methods

### 2.1 Materials

Apple fruits (*Malus domestica* 'Elstar' and 'Pinova') have been harvested in the orchard near Glindow (Germany). The middle of the field was located at latitude 52°N 22' 14.96" and longitude 12°E 52' 22.69". The selected area of 25×150 m had North-West to South-East orientation and was split into upper and lower part according to the position of a hill inside. Soil was drier and trees were obviously smaller within the area of the hill. Both upper and lower regions were split into two parts for cultivars 'Elstar' and 'Pinova'. Four rows and 100 trees were used to collect fruits from each quarter of 12.5×75 m. Harvested fruits were classified into the commercial grades of unripe, ripe and overripe by people working on the harvest. Although those people do not make a certified sensory panel, they have several years experience in manual quality assessment. Harvested fruits were transferred into the storage facility immediately. Separate chambers were provided for apples of the same ripeness stage and cultivar. Temperature was adjusted to 2°C. The atmosphere inside chambers consisted of 2% CO<sub>2</sub> and 1.5% O<sub>2</sub>. This controlled atmosphere cool storage started in August 2008 and took 157 and 164 days for 'Elstar' and 'Pinova', respectively. The continuous storage was broken for a few minutes in order to perform the measurements in 22 and 24 cases for 'Elstar' and 'Pinova', respectively. For one measurement, 30 pieces of apple were randomly selected. The total amount of 2799 images was investigated during the experiment (**Table 1**).

**Table 1:** Composition of apple sample (number of images taken)

Ripeness stage	Location within orchard		Total
	Upper	Lower	
Apple of 'Elstar'			
Unripe	232	236	468
Ripe	210	206	416
Overripe	239	240	479
Apple of 'Pinova'			
Unripe	238	234	472
Ripe	240	240	480
Overripe	242	242	484

## 2.2 Vision system

Digital images of 720×576 pixel size and 0.1694 mm/pixel resolution were acquired. Measurements took place in a darkroom in order to maximize signal to noise ratio. The vision system was consisted of a monochrome camera (JAI A50IR CCIR, JAI, Denmark), zoom lenses (model H6Z810, PENTAX Europe GmbH, Germany), external analog video converter (VRM AVC-1, Stemmer Imaging GmbH, Germany) and a laser module (LPM785-45C, Newport Corp., USA) emitting at 785 nm with 45 mW power. The camera and laser module were aligned in 0/7° geometry. The acquisition process was controlled by LabView 8.6 PDS software (National Instruments, USA) extended with a dynamic library of specific image processing functions.

## 2.3 Estimation of optical parameters

The incident point was automatically identified as the mass point of the highest intensity area. The intensity values of the illuminated region were collected with radial averaging relative to the incident point. The shapes of these profiles were compared to the results of Monte Carlo simulation in order to estimate anisotropy factor ( $g$ ) and total interaction coefficient ( $\mu_t$ ,  $\text{cm}^{-1}$ ). Simulations were run with the optical parameters of  $\mu_a=0.63 \text{ cm}^{-1}$ ,  $\mu_s=30 \text{ cm}^{-1}$  and  $g=0-0.99$ . The refractive index of  $n=1.35$  was assumed for apple tissue. The profiles were found to rotate as a result of changing anisotropy factor and the decline of measured intensity may be used to estimate the value of this optical property (BARANYAI & ZUDE 2008). Trigonometric function (Eq. 1) was found to describe well ( $r^2=0.9995$ , Durbin-Watson  $D=2.0293$ ) the relationship between slope of the logarithmic profiles and anisotropy factor.

$$y = a + b \cdot \tan\left(x \frac{\pi}{c}\right) \quad (1)$$

The average diameter of the backscattering area at 50% intensity level (FWHM) was computed based on the diffusion theory model and its correlation with optical parame-

ters was investigated (**Table 2**). The best correlation was found with the total interaction coefficient ( $\mu_t = \mu_a + \mu_s'$ ).

**Table 2:** Correlation between optical parameters and FWHM

Correlation	$\mu_a$	$\mu_s'$	$\mu_t$	$\mu_{\text{eff}}$
Pearson (linear)	-0.0475	-0.8645	-0.8653	-0.6828
Spearman (rank)	-0.0393	-0.9990	-0.9996	-0.7354

From practical point of view, the effective attenuation coefficient ( $\mu_e = [3\mu_a(\mu_a + \mu_s')]^{1/2}$ ) is very important since its reciprocal value describes the theoretical penetration depth (QIN & LU 2009). The optical parameters were adjusted in a wide range of  $\mu_a = 0.004\text{--}0.63\text{ cm}^{-1}$ ,  $\mu_s' = 3.2\text{--}35\text{ cm}^{-1}$  in order to find a suitable model. **Figure 1** shows that the total interaction coefficient might be estimated better due to the lower deviations.

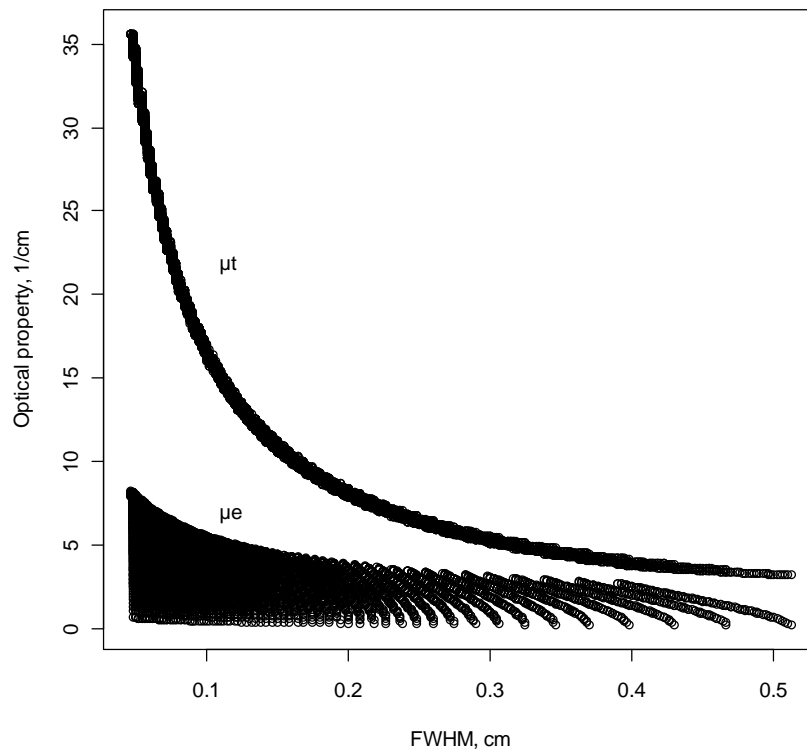


**Figure 1:** Relationship between backscattering spot size (FWHM), effective attenuation ( $\mu_e$ ) and total interaction ( $\mu_t$ ) coefficients

The reciprocal function fitted well to the  $10^4$  data points with  $r^2=0.998$ . The root mean square error of prediction (RMSEP) was  $0.37\text{ cm}^{-1}$  using 10% randomly selected data in 100 repetitions.

The 25% intensity level between minimum and maximum backscattering signal was also calculated. The elliptical distortion of the position of equi-intensity pixels at this level was computed. The ratio of radii measured in perpendicular directions was found to de-

scribe the proportion of reduced scattering coefficients and structural anisotropy (SVIRIDOV *et al.* 2005). The distortion of the circular laser beam is 0.751% on plain surface at 7° incident angle. This offset value was used to correct calculated ratios.

### 3 Results and discussion

The estimated values for total interaction coefficient ( $\mu_t$ ) are presented in **Figure 2**. The error bars represent the 95% confidence interval of mean values for each day of measurement. The estimated values for unripe, ripe and overripe pieces were more similar for 'Pinova' apples than that of 'Elstar'. Observed values changed up to 15% during storage. The curves for unripe and overripe pieces run parallel until the 81<sup>th</sup> day of storage, beginning of December 2008, when break occurs in the trend. All groups of apples show this dual behaviour which may indicate that  $\mu_t$  estimated at 785 nm was also affected by attributes other than firmness. However, similar non-linear relationship was observed between textural acceptability and firmness of apples during storage (KONOPACKA & PLOCHARSKI 2004). The analysis of variances (ANOVA) revealed that estimated values were primarily affected by the storage time, position in the orchard and cultivar, in this order.

The estimated values for anisotropy factor ( $g$ ) are presented in **Figure 3**. The error bars represent the 95% confidence interval of mean values for each day of measurement. Estimated values change in a narrow band, less, than 2.1%. Each sample group had negative correlation between storage time and anisotropy factor. It means that the effect of general scatterers present in the tissue was slightly decreased. Pieces belonging to the ripe class obtained the lowest correlations for both cultivars. The anisotropy factor, and the gradient of the outline of the backscattering area, changed the most for overripe pieces of 'Elstar' and unripe pieces of 'Pinova'. According to the ANOVA results, estimated values of anisotropy factor were primarily affected by the storage time and ripeness stage, in this order. The analysis of interaction effects confirmed that pieces belonging to different ripeness stages change anisotropy factor with different pace.

The basic statistical parameters of elliptical distortion of the diffusively illuminated area are presented in **Table 3**. The mean value of 1.119 and the distribution of measured data around mean do not show significant distortion. This result indicates that apples did not have significant internal structures. Typical fibrous biological materials, such as human skin or demineralised bone, result in the ratio above 1.5 (SVIRIDOV *et al.* 2005).

**Table 3:** Statistical parameters of elliptical distortion of illuminated area

Mean	1 <sup>st</sup> quartile	Median	3 <sup>rd</sup> quartile	Std. deviation
1.119	1.083	1.112	1.144	0.049

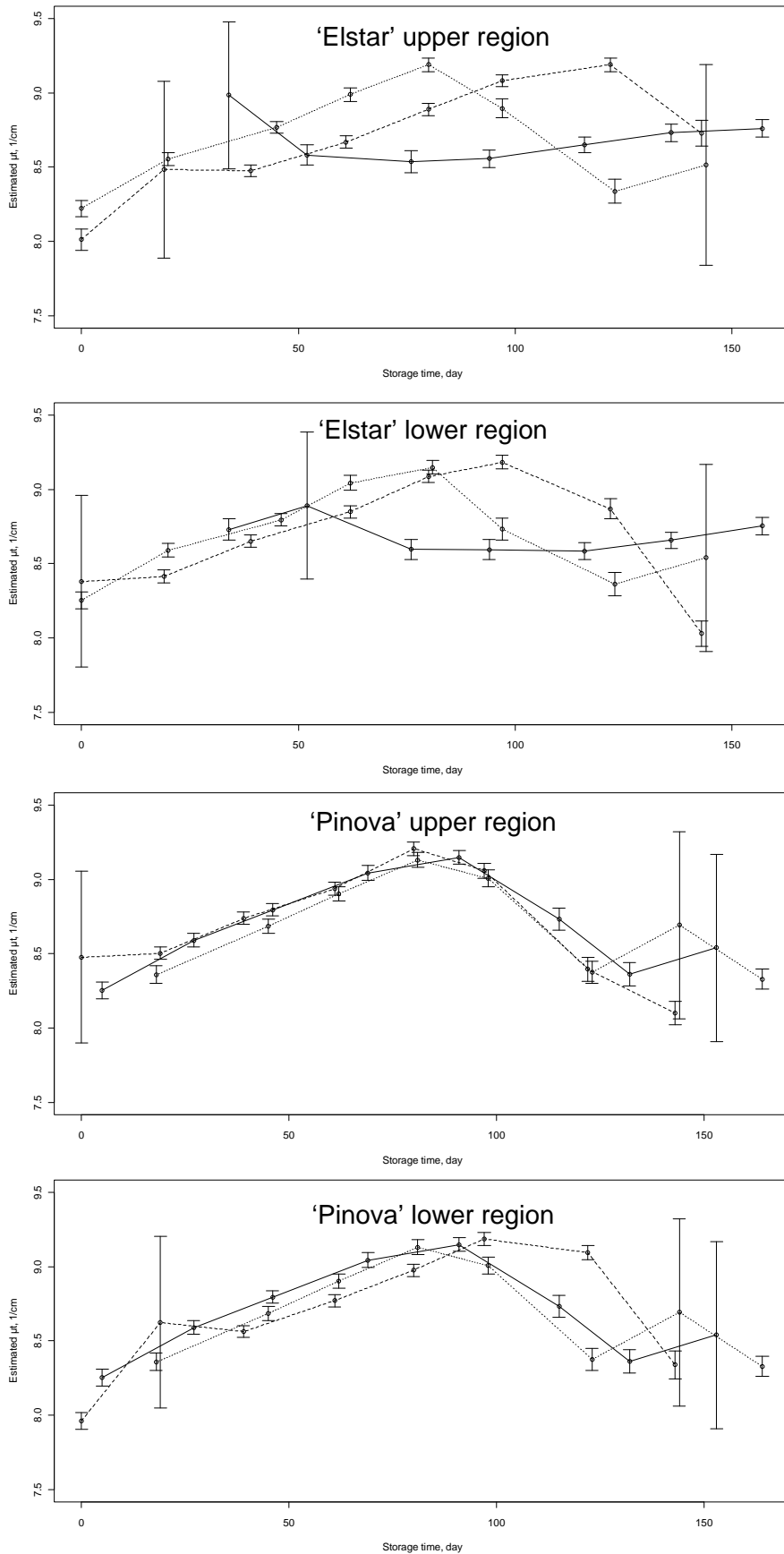


**Figure 2:** Changes in total interaction coefficient during controlled atmosphere cool storage (..... overripe, — ripe, - - unripe)

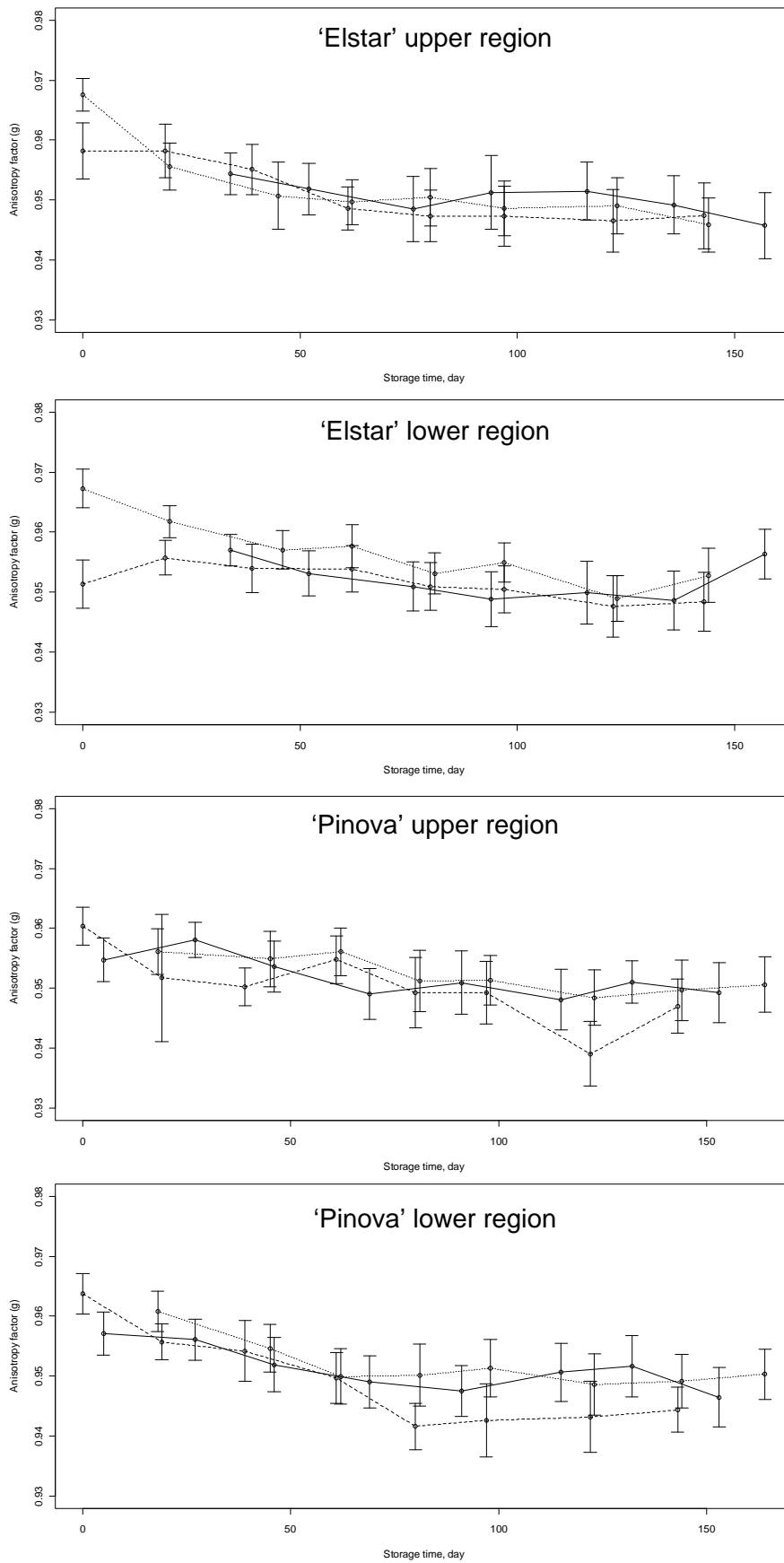


**Figure 3:** Changes in anisotropy factor during controlled atmosphere cool storage (.... overripe, — ripe, - - unripe)

## 4 Conclusions

Laser induced diffuse reflectance (backscattering) imaging technique was used to monitor selected optical properties of 'Elstar' and 'Pinova' apples during controlled atmosphere cool storage. The total interaction coefficient ( $\mu_t$ ,  $\text{cm}^{-1}$ ) and anisotropy factor ( $g \in ]-1, 1[$ ) were estimated on the basis of spatial intensity distribution. The total interaction coefficient was found to increase significantly within the first 81 days and decrease afterwards. The observed break in the trend indicates that  $\mu_t$  estimated at 785 nm might be affected by more parameters additionally to firmness. Similar behaviour was found in the literature for texture acceptability. The statistical analysis pointed out that observed values were mainly affected by the storage time, position in the orchard and cultivar, in this order. Almost monotonous decrease was observed in case of anisotropy factor. The change in anisotropy factor was less (2.1%) than that of in total interaction coefficient (15%). Analysis of variances revealed that mainly storage time and ripeness stages affected estimated values, in this order. The elliptical distortion of the visible backscattering signal at 25% intensity level was also investigated to determine whether significant internal structures occur or change in the tissue. The comparison of results to literature data did not predict directional structures in apple.

The presented image processing method might be used to describe and monitor optical properties of apples and other fruits during storage and provide additional information for quality assurance rapidly.

## References

- BARANYAI L., ZUDE M. (2008):** Analysis of laser light migration in apple tissue by Monte Carlo simulation. *Progress in Agricultural Engineering Sciences*, 4: 45-59
- ELMASRY G., WANG N., VIGNEAULT C. (2009):** Detecting chilling injury in Red Delicious apple using hyperspectral imaging and neural networks. *Postharvest Biology and Technology*, 52: 1-8
- KIM K.-B., LEE S., KIM M.-S., CHO B.-K. (2009):** Determination of apple firmness by nondestructive ultrasonic measurement. *Postharvest Biology and Technology*, 52: 44-48
- KONOPACKA D., PLOCHARSKI W.J. (2004):** Effect of storage conditions on the relationship between apple firmness and texture acceptability. *Postharvest Biology and Technology*, 32: 205-211
- LIU Y., YING Y. (2005):** Use of FT-NIR spectrometry in non-invasive measurements of internal quality of 'Fuji' apples. *Postharvest Biology and Technology*, 37: 65-71
- SVIRIDOV A., CHERNOMORDIK V., HASSAN M., RUSSO A., EIDSATH A., SMITH P., GANDJBAKHCHE A.H. (2005):** Intensity profiles of linearly polarized light backscattered from skin and tissue-like phantoms. *Journal of Biomedical Optics*, 10(1), 014012/1-9
- QIN J., LU R. (2008):** Measurement of the optical properties of fruits and vegetables using spatially resolved hyperspectral diffuse reflectance imaging technique. *Postharvest Biology and Technology*, 49: 355-365
- QIN J., LU R. (2009):** Monte Carlo simulation for quantification of light transport features in apples. *Computers and Electronics in Agriculture*, 68: 44-51
- XING J., BRAVO C., MOSHOU D., RAMON H., DE BAERDEMAEKER J. (2006):** Bruise detection on 'Golden Delicious' apples by vis/NIR spectroscopy. *Computers and Electronics in Agriculture*, 52: 11-20